Separation and Purification Technology 194 (2018) 319–328

Contents lists available at ScienceDirect

Separation and Purification Technology

journal homepage: www.elsevier.com/locate/seppur

Nanofiltration of indium and germanium ions in aqueous solutions: Influence of pH and charge on retention and membrane flux

Arite Werner[a,*], André Rieger[a], Maria Mosch[a], Roland Haseneder[a], Jens-Uwe Repke[a,b]

[a] TU Bergakademie Freiberg, Institute of Thermal, Environmental and Natural Products Process Engineering, 09596 Freiberg, Germany
[b] TU Berlin, Process Dynamics and Operations Group, 10623 Berlin, Germany

ARTICLE INFO

Keywords:
Nanofiltration
Zeta potential
Speciation
Indium
Germanium

ABSTRACT

The retention of $In_2(SO_4)_3$ and GeO_2 with two different commercially available polymeric nanofiltration (NF) flat sheet membranes (NP010, NF99HF) was investigated between pH 2 and 12. The main objective of this experimental study is to investigate the selective separation of both indium and germanium in aqueous sulfate solution. The experiments focus on a future membrane application for winning indium and germanium from bioleaching solutions. The investigation was conducted with synthetic solutions while single salt experiments and experiments with the binary salt system were performed. Depending on pH value, ions show different speciation which strongly influences membrane charge and separation performance. Streaming potential measurements with $In_2(SO_4)_3$ and GeO_2 were performed to determine zeta potential as a measure of membrane charge. KCl was used as a reference system of zeta potential since it is considered inert regarding interaction with the membrane surface. Both, zeta potential profiles of single salt solutions and binary mixtures showed a remarkable interaction between indium and germanium ions and the membrane surface because the IEP was shifted to a higher pH value. The results were ascribed to specific adsorption of In^{3+} on the membrane surface. The nanofiltration experiments revealed that indium and germanium are separated successfully within distinct pH values which is caused by electrostatic interaction of species like In^{3+} and $In(OH)_4^-$ and the membrane charge. Furthermore, size exclusion plays a distinctive role in the separation of $In(OH)_3^0$ and $Ge(OH)_4^0$. Above all, we could show that germanium can successfully be enriched in the permeate.

1. Introduction

The use of metals in high tech applications has increased strongly in recent decades. The main reasons for this development are an increasing global population as well as new technologies needed for modern communication and information technology. Consequently, the European Commission initiated an evaluation to define critical raw materials for the European Union's economy. In 2013 fifty-four raw materials have been analyzed and finally twenty were identified as critical. The list also includes indium and germanium. The main reasons are their economic importance as well as an existing supply risk because worldwide production is dominated by China. Therefore, the European Union is highly dependent on importing ores from which indium and germanium are produced. More critical aspects are low recycling rates and mostly no alternatives for substituting indium and germanium through other non-critical elements. While the global primary production of germanium was 160 tons per year in 2015 the demand is predicted to increase up to 200 tons per year in 2030 [1–3]. Main applications of germanium are the production of fiber optic cables and products for IR-optics. The global primary production of indium is stated to be 759 tons per year in 2015. Until 2030 it is predicted to increase up to 1911 tons per year. Indium is mainly used for the production of liquid crystal displays (LCD) and thin-film photovoltaics [4–6].

Since indium and germanium are enriched in zinc sulfide ores (sphalerite, ZnS), the common method of winning is as a by-product of zinc production via pyro- and hydrometallurgy [7]. Beside the conventional winning methods, bioleaching of metal ores is an effective method to extract metals from low-grade ores and forms the basis for the current work. It is an environmentally friendly technology since no harmful organic solvents have to be used. Furthermore low operating costs are needed, so it is compatible with the requirements to be implemented at commercial scale [8]. Through microbial activity of acidophilic bacteria (e.g. *Acidithiobacillus ferrooxidans*) sulfide is oxidized to either sulfur or sulfate while zinc and further metal ions are mobilized and transferred into aqueous solution [9,10]. The bioleaching solution to be treated is characterized by a variety of high concentrated metal ions in sulfate dominated aqueous solution,

* Corresponding author.
E-mail address: arite.werner@tun.tu-freiberg.de (A. Werner).

https://doi.org/10.1016/j.seppur.2017.11.006
Received 28 June 2017; Received in revised form 22 October 2017; Accepted 2 November 2017
Available online 04 November 2017
1383-5866/

whereas indium and germanium are low concentrated. To provide an effective downstream processing for separating indium and germanium from the leaching solution, solvent extraction and membrane technology are aimed to be linked together. In this paper the potential of polymeric nanofiltration (NF) membranes for removing indium and germanium from synthetic aqueous solution is investigated preliminary to the treatment of real leaching solutions. NF is a pressure driven membrane process. Its common application is the purification of water (e.g. remove hardness) and fractionation of ions and small molecules in a variety of industries due to its ability to separate univalent from polyvalent ions [11].

Separation mechanisms between polymeric NF membranes and electrolyte solutions remarkably depend on membrane characteristics and solution composition. It mainly includes steric and electrostatic partitioning between the membrane and the electrolyte solution as well as sorption effects due to different affinity between the ions and the membrane material [12,13]. The membrane surface is characterized by the appearance of hydrophobic and hydrophilic functional groups. In contact with electrolyte solutions a surface charge is acquired because of different interactions [14]. The most important are dissociation of hydrophilic functional groups, specific and unspecific adsorption of ions on hydrophobic groups and the adsorption of polyelectrolytes, ionic surfactants and charged macromolecules [15,16]. Altering the pH value also changes the membrane charge since surface functional groups dissociate. The pH value at which the membrane has no net charge is known as the isoelectric point (IEP). Commonly, NF membranes show an IEP in a pH range 3–6. Hence, they are positively charged in acidic pH-range and negatively charged for neutral to alkaline conditions [17]. In general polymeric membranes show amphoteric behavior [18–20]. The charged membrane surface affects ion retention due to electrostatic interaction which in turn is related to the ions present in solution [21]. Ions can occur in different chemical species which have an effect on charge, solubility and diffusion coefficient. Consequently ion speciation directly affects membrane transport. Regarding metal ions, complex reactions with different ligands in solution have to be considered. In the metal-ligand-system speciation depends on several factors like pH, ionic strength and redox conditions [22,23].

Fig. 1 shows the calculated speciation diagrams of indium and germanium hydrolysis. The stability constants have been critically reviewed and summarized by Baes and Mesmer [24] and hence provide reliable information which is convenient for reference.

The most important oxidation state of indium is III. The hydrated In^{3+} is coordinated with six water molecules with a bond distance In−OH_2 of 2.15 ± 0.03 Å and therefore exists as octahedral complex $[In(H_2O)_6]^{3+}$. For the following consideration it is simplified and expressed in terms of In^{3+}. At ambient temperature, In^{3+} is most likely predominant at pH less than 4. Indium occurs in water as mononuclear (poly-)hydroxides like $In(OH)^{2+}$, $In(OH)_2^+$, $In(OH)_3^0$ and $In(OH)_4^-$ whereas $In(OH)_3^0$ and $In(OH)_4^-$ (Fig. 1a) are predicted to be the most dominant species in the absence of other ligands within neutral and alkaline pH-range. There is also evidence of occurring indium sulfate species [26]. Consequently the availability of sulfate will modify the speciation diagram.

Germanium occurs in the oxidation states II and IV. Because redox potential of natural environments is too high, divalent species rarely occur [27]. The most important species in aqueous solution are germanic acid $Ge(OH)_4^0$ and its dissociation products $GeO(OH)_3^-$ and $GeO_2(OH)_2^{2-}$ (Fig. 1b). The latter occurs in slightly alkaline solution. In contrast to indium, the single cation Ge^{4+} rarely exists although its occurrence is discussed in literature for highly acidic solution [26].

The separation of metal ions with NF membranes depending on pH-value is a major issue. Hoyer et al. [28] investigated the separation of uranium species with NF membranes from mining waters depending on pH value. Cross-flow experiments revealed uranium retention of more than 99% which lead to a considerable reduction from 1.6 mg l^{-1} to 3 µg l^{-1} uranium in the mine effluent. Further studies about the separation of $Pb(NO_3)_2$ and $Co(NO_3)_2$ with NF polyamide membranes have been performed by Bouranene et al. [29]. They varied the pH value between pH 3 and 7 and a distinct influence of pH value on retention was observed. For instance, in single-salt solutions, retention of lead was higher compared to copper at pH ≥ 5. Because this result does not agree with stokes radii of lead and copper ions, steric effects were excluded while membrane ion interaction were supposed to be the leading separation mechanism. Gherasim et al. [30] studied the removal of Pb^{2+} and Cd^{2+} from synthetic solutions made of $Pb(NO_3)_2$ and $Co(NO_3)_2$ under variable operating conditions while changing the pH value in a range between pH 3 and 5.7. In a single salt solution of $Pb(NO_3)_2$ the retention of Pb^{2+} increased with increasing pH due to electrostatic interaction between the lead ions and the charged membrane surface. In binary salt solutions, a correlation between metals hydration energies and retention of the metal ions was detected. The separation of indium chloride with three different NF membranes has been investigated in literature under various operating conditions in cross flow mode [31]. The pH value was adjusted to pH 6 and 8 which enhances indium retention. This observation was ascribed to the formation of indium hydroxide and aquo-cation complexes in the presence of Na^+ and Cl^- above pH 7. The retention behavior at pH 6 was assumed to be due to the formation of indium oxide complexes. Since indium forms reasonably stable chloride complexes [26] which in turn affect occurring speciation, these results are not applicable to the current sulfate system.

The purpose of the current work is giving a detailed experimental basis for a future technological application, namely separating indium and germanium from leaching solutions coming from a bioleaching application. Therefore a series of experiments were designed to evaluate the influence of pH value, concentration of the solutes and the application of dead end or cross flow mode. First of all, the performance

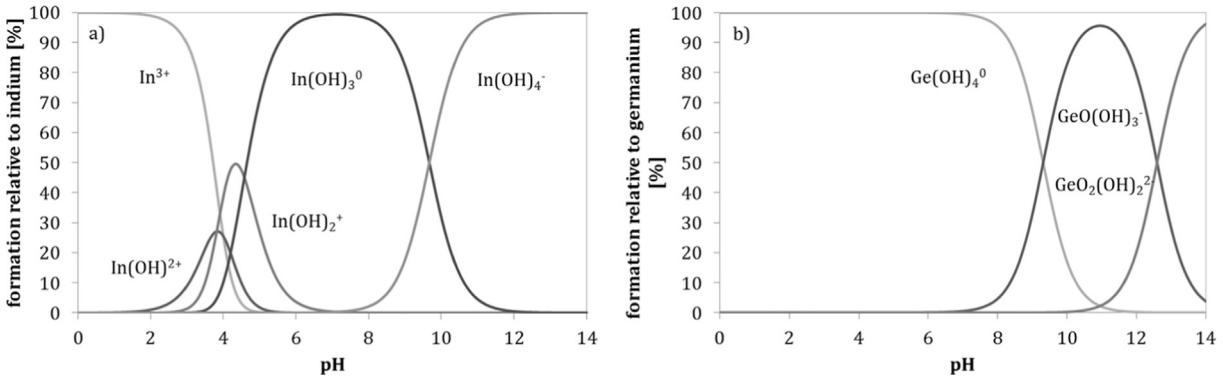

Fig. 1. Speciation diagrams of (a) 1 mmol l^{-1} indium in water and (b) 1 mmol l^{-1} germanium in water (calculation with software HySS using stability constants from Baes and Mesmer [24,25]).

Table 1
Nanofiltration membrane properties [34,35].

Membrane	NF99HF	NP010
Supplier	Alfa Laval	Microdyn Nadir
Membrane material	Polyamide thin film composite on polyester support	Polyethersulfone
Recommended operating conditions:		
pH range	3–10	0–14
Processing temperature [°C]	5–50	5–95
Maximum operating pressure [bar]	55	40
Main characteristics:		
MWCO [Da]	200	1000
Pure water flux [l m^{-2} h^{-1}]	324 ± 32[a,b]	230 ± 57[a,b]
Nom. retention [%]	Na_2SO_4: 99[a] $MgSO_4$: > 98	Na_2SO_4: 35–75 $MgSO_4$: 15[a]
Mean pore radius	0.43 nm[c]	1.33 nm[d]
Isoelectric point	4.12–4.42[c] (10 mmol l^{-1} KCl)	5.3[e] (1 mmol l^{-1} KCl) < 3.5[f]) (1 mmol l^{-1} KCl)

[a] 15 bar, 20 °C, stirred vessel, 500 min^{-1}.
[b] Arithmetic mean ± standard deviation.
[c] [36].
[d] [37].
[e] [38].
[f] [39].

of two different NF membranes, used for the removal of indium and germanium ions from synthetic aqueous solutions are presented in this paper, with particular focus on pH-variation. By using different polymeric NF membranes we want to evaluate the influence of different membrane material on the overall membrane performance. The influence of single salt solutions as well as binary salt mixtures on retention, permeate flux and membrane surface charge were experimentally investigated.

2. Experimental work

2.1. Membranes and chemicals

After a preliminary screening with five different commercial NF flat sheet membranes, NF99HF and NP010 were selected for detailed testing because they showed the best performance regarding permeate flux and ion retention [32,33]. Membrane characterization is listed in Table 1. Unmarked information was given by the manufacturer. The feed solution contained 10 mg l^{-1} GeO_2 (purity 99.9999%; Alfa Aesar) and 10 mg l^{-1} $In_2(SO_4)_3$ (purity 99.99%; ChemPUR). All of the aqueous solutions were prepared by using ultrapure water (conductivity < 0.055 µS cm^{-1}). The pH value of aqueous solution was adjusted by dosing appropriate amounts of H_2SO_4 and NaOH, respectively.

2.2. Zeta potential measurements

To evaluate the effect of indium and germanium ions on the value and sign of the membrane charge, the pH dependent zeta potential of the membrane surface was determined by measuring the streaming potential. Prior to the measurements the membranes were conditioned with Ultrasil® (15 g l^{-1}) for 45 min. Afterwards they were stored in deionized water. The measurements were performed with the SurPASS™ electrokinetic analyzer (Anton Paar GmbH, Austria) employing an adjustable gap cell for disks. The sample size was 13 mm in diameter. Experiments were performed twofold. For each experimental run, a new membrane coupon was used. To reveal the effect of specific interaction between the membrane surface and complex solutions of indium and germanium, a comparison with KCl (p.a., Merck) solution was done. Therefore two different electrolyte solutions were investigated for the zeta potential measurements: 1 mmol l^{-1} KCl as well as single-salt solutions and binary mixtures of 10 mg l^{-1} GeO_2 (purity 99.9999%; Alfa Aesar) and 10 mg l^{-1} $In_2(SO_4)_3$ (purity 99.99%; ChemPUR).

KCl was used as a reference system because it is inert regarding membrane surface interaction [40]. Aqueous solutions of indium and germanium were investigated to consider the effect of different ion speciation on zeta potential. The pH was adjusted in a range of pH 3–8 by titration of H_2SO_4 (0.05 mol l^{-1}) and NaOH (0.05 mol l^{-1}) respectively. The pressure difference along the streaming channel was 300 mbar. The average gap height was adjusted to 97 ± 2 µm which results in a flow rate of 100 ml min^{-1}. The measurements were performed at ambient temperature. Prior to the measurements the system was rinsed with feed solution which is rejected before starting the streaming potential measurement. The SurPASS™ software Visiolab calculated the zeta potential by using the Helmholtz-Smoluchowski equation (see Eq. (1)) [15]

$$\zeta = \frac{\Delta U}{\Delta p}\frac{\eta}{\varepsilon_0 \varepsilon}\frac{L}{A}\frac{1}{R} \quad (1)$$

where ΔU is the measured streaming potential, Δp is the applied pressure, η the viscosity of the solution, ε the dielectric permittivity of the solution, ε_0 the permittivity of vacuum, L/A the cell constant and R the electrical resistance inside the streaming channel, respectively.

2.3. Nanofiltration experiments

Nanofiltration experiments were conducted to investigate the pH-dependent retention of indium and germanium by means of single salt solutions and binary mixtures. The experiments were performed in dead end filtration mode illustrated in Fig. 2.

The membrane surface area was 34 cm^2 and the temperature was maintained at a constant value of 25 °C using a heat exchanger. The membrane sheet was placed on a porous sinter disc to avoid mechanical damage during the experiment. The feed volume was 450 ml. To prevent concentration polarization, the experiments were conducted under stirring conditions. The stirring speed was set to 500 rpm. The batch vessel was pressurized with N_2 at 15 barg. Comparable to the zeta potential measurements, the flat sheet membranes were conditioned with Ultrasil® (15 g l^{-1}) for 45 min, subsequently stored in deionized water for one hour and finally in feed solution. The single salt experiments were repeated twice, those with binary salt mixtures were repeated four times. Prior to the use of a new membrane sheet the pure water flux was determined. The experiments were performed in a broad pH range of 2, 3, 4, 5, 6, 7, 8 and 12 to investigate the influence of alternating ionic species and a changing membrane surface charge on the separation performance. The membrane sheet was replaced after the complete pH range was measured. Conductivity and pH-value were determined before and after the experiments. Between two consecutive experiments the membrane was flushed with 200 ml of deionized water. The mass of permeate was recorded over the duration of the experiment. When a permeate mass of 200 g was accumulated on the laboratory balance, the experiment was immediately stopped and 10 ml samples of permeate and retentate were taken. To evaluate the separation performance of the polymeric NF membranes the observed retention $R_{i,obs}$ was calculated according to Eq. (2), where m_{Pi} and m_{Ri} are the mass of permeate and retentate, respectively.

$$R_{i,obs} = \left(1 - \frac{m_{P_i}}{m_{R_i}}\right) \quad (2)$$

An adapted measure of retention of indium and germanium was applied by using the ratio of the mass of solute in permeate and retentate (see Eq. (2)), respectively. An adaption of the usual definition of retention

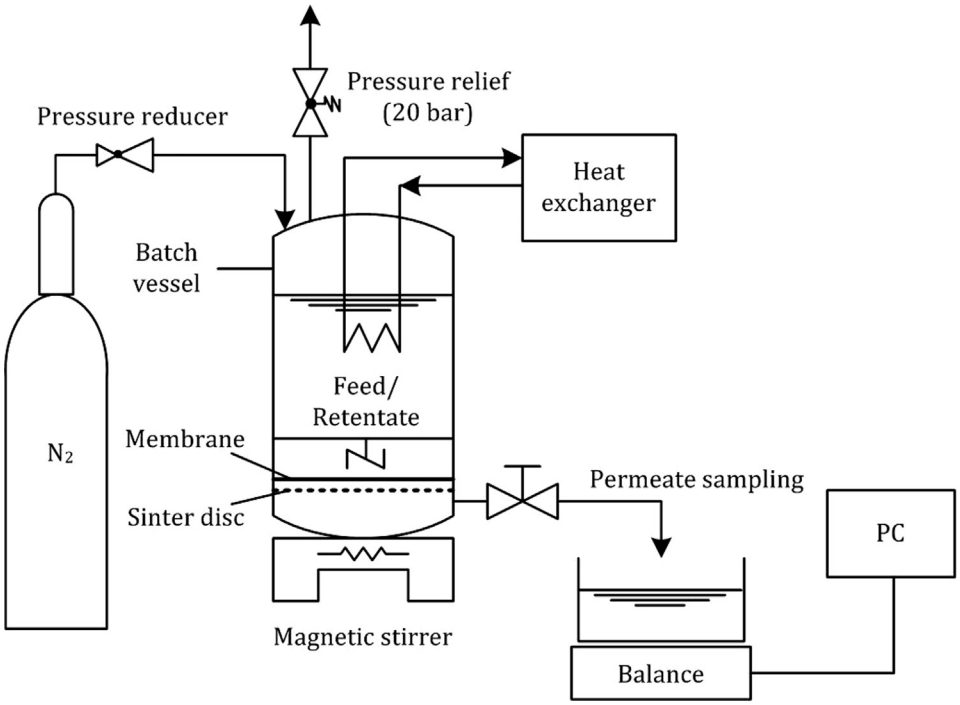

Fig. 2. Experimental set-up of nanofiltration experiments in dead end mode.

employing concentrations seemed reasonable, since concentration of the feed solution constantly changes due to static filtration during dead end filtration mode. Furthermore, retention based on concentration values has been derived for steady-state processes such as of cross flow filtration.

2.4. Analytical methods

The elemental analysis of indium and germanium in samples of feed solution, permeate and retentate was determined via ICP (inductively coupled plasma) MS (mass spectrometer) (ICP-MS Elan 9000, Perkin Elmer SCIEX). The device was equipped with a microflow nebulizer (PFA-ST Nebulizer) and a baffled quartz cyclonic spray chamber (both AHF analysentechnik AG, Tuebingen, Germany). The atomic mass used for determination was 113 for indium and 74 for germanium, respectively. 10 $\mu g\,l^{-1}$ Rhodium was used as internal standard. The pH value (model "SenTix® 940") and conductivity (model "TetraCon® 925") of the solutions were measured with a multi parameter portable meter (Multi 3420 Set C, WTW, Germany).

3. Results and discussion

3.1. Zeta potential measurements

3.1.1. Zeta potential measurements with *KCl*

Evaluation of the initial membrane charge of the utilized polymeric NF membranes, streaming potential measurements were performed by using 1 $mmol\,l^{-1}$ *KCl*. The measured zeta potential values for NF99HF and NP010 are shown in Fig. 3. The measurements were performed between pH 2 and 9. Error bars in y-direction illustrate maximum and minimum values of two experiments. This nomenclature is consistently used for all zeta potential diagrams.

Polymeric polyamide membranes often show amphoteric behavior and consequently a pH-dependent surface charge. They are positively charged at low pH. With increasing pH, the IEP is passed and positive charge switches into negative charge [41]. At the IEP the membrane has no net charge. As Fig. 3 shows, the IEP of NF99HF is revealed between pH 2.1 and 2.3. With increasing pH value, the zeta potential decreases. The zeta potential curve of NF99HF shows a typical amphoteric

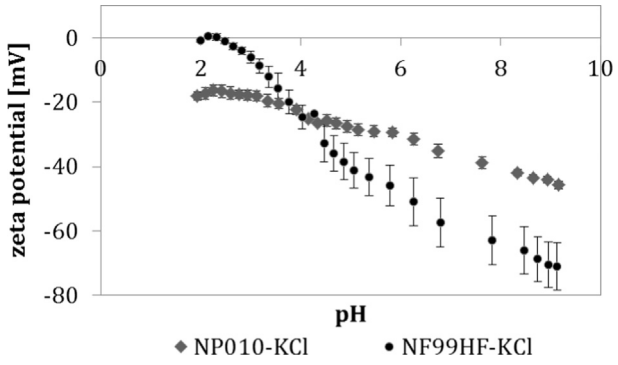

Fig. 3. NF99HF and NP010. Results of zeta potential measurements for aqueous solutions of 1 $mmol\,l^{-1}$ KCl.

behavior, which is mentioned above. The active layer of NF99HF is made of polyamide (see Table 1), so amine groups ($-NH_3^+$) and carboxylic groups (−COOH) are located at the membrane surface. Carboxylic groups are weakly acidic and therefore dissociating at higher pH to form $-COO^-$ [42]. The more alkaline amine groups are positively charged at low pH-values due to protonation ($-NH_3^+$) [15]. Consequently, polyamide membranes acquire a positive surface charge at low pH and a negative surface charge at high pH values because carboxylic groups are deprotonated. The obtained IEP is lower compared to the findings acquired in literature (see Table 1). The experimental deviation in the experiments is attributed to the variability of the intrinsic membrane characteristic since a new membrane sample was used for each measurement.

Unlike the NF99HF membrane, zeta potential of NP010 shows different behavior. Results show that NP010 is negatively charged throughout the investigated pH range (see Fig. 3). This is in contrast to the IEP found in literature (see Table 1). However the permanent negative surface charge goes along with the membrane material (see Table 1). Occurring sulfonic groups ($-SO_3^-$) are strongly acidic and dissociated over a wide pH range [42]. Consequently, the membrane surface is negatively charged within the entire pH scale as results for NP010 indicate (Fig. 3). The NF99HF membrane shows a steeper zeta potential profile compared to NP010. Also the membrane charge is

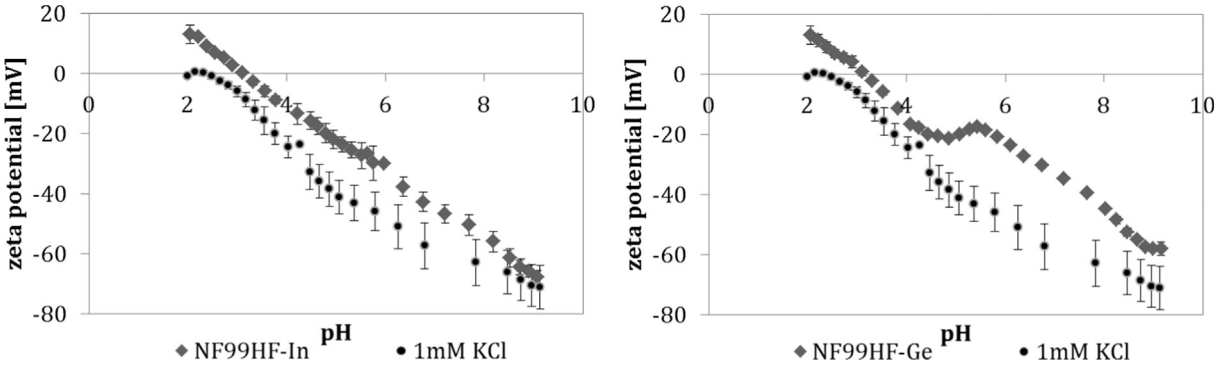

Fig. 4. NF99HF. Results of zeta potential measurements for single salt aqueous solutions of 10 mg l^{-1} $In_2(SO_4)_3$ (left) and 10 mg l^{-1} GeO_2 (right) compared to 1 mmol l^{-1} KCl.

noticeably more negative which implies a higher density of negative functional groups [14,15]. The differences in the zeta potential curves clearly represent the differences in surface chemistry of the membranes.

3.1.2. *Effect of* $In_2(SO_4)_3$ *and* GeO_2 *on membrane surface charge – single salt solutions*

For identification of the specific interaction between ions of indium and germanium and the membrane surface, differences between zeta potential of single salt solutions and KCl were evaluated. The comparison with KCl solution is consistently done for all the following results dealing with zeta potential. Fig. 4 shows the results of the NF99HF membrane.

In comparison to the KCl measurements, the zeta potential of the NF99HF membrane changes when it is in contact with the single salt solutions of indium and germanium, as Fig. 4 demonstrates. In case of the indium solution (see Fig. 4, left) the IEP is shifted towards pH 3.1 which indicates specific adsorption of In^{3+} on the membranes surface due to the positive shift of the IEP [14]. The overall trend of the zeta potential represents the behavior of a polyamide membrane (see Section 3.1.1). When the membrane is in contact with the single salt solution of germanium (see Fig. 4, right), also a positive shift of the IEP towards pH 3.4 is detected. Unlike indium, germanium does not occur as a cation but as uncharged $Ge(OH)_4^0$ and hence will not adsorb at the membrane surface. So this observation remains unclear. In addition, the zeta potential profile of germanium shows a wavy segment between pH 4 and 6. In [40] we found a similar course of a zeta potential curve which was attributed to swelling of the charged polymeric material. The hypothesis is, that dissociating negatively charged surface functional groups and a subsequent repulsion between adjacent and equally charged functional groups, lead to an expansion of the polymer chains. Hence, swelling of the material is induced which increases accessibility of the electrolyte solution to the functional groups located at the inner surface. Finally, it leads to an introduction of ionic conductance in the polymeric material which causes a short-term increase in zeta potential. Since the NF99HF contains negatively charged functional groups, the hypothesis might be applicable but needs to be verified by further experiments.

The zeta potential curves for NP010 membrane using single salt solutions of indium and germanium are shown in Fig. 5.

Electrolyte solutions of indium and germanium cause a shift of the NP010 zeta potential curves towards more positive values when compared to the KCl experiments. This result is comparable to NF99HF. According to the membrane material polyethersulfone (see Table 1) a negative membrane surface charge would be expected throughout the whole pH range (see Section 3.1.1). Since an IEP is detected, this result must be related to the specific adsorption of cations onto the membrane surface. Consequently we can point out that NF99HF and NP010 show specific interaction with aqueous solutions of indium and germanium. The experiments with single salt solutions of indium sulfate reveal an IEP at pH 2.3 (see Fig. 5, left). The results can again be attributed to a specific adsorption of In^{3+} on the membrane surface. The IEP obtained with the single salt solution of germanium reveal an IEP at pH 2.1 which again is not in accordance with the speciation of germanium. Hence, specific adsorption due to ionic interaction with the membrane surface can be excluded due to the occurrence of the uncharged $Ge(OH)_4^0$. Both curves show a similar trend with a wavy segment between pH 4–6. A possible explanation for this observation is given above.

3.1.3. *Effect of* $In_2(SO_4)_3$ *and* GeO_2 *on membrane surface charge – binary mixtures*

To evaluate the effect of indium and germanium ions in combined solution, experiments with binary mixtures were performed. Fig. 6 shows the results for the NF99HF membrane.

The measurements with the binary mixture of $In_2(SO_4)_3$ and GeO_2 revealed the IEP at pH 3.5. If the results are compared to the results obtained with single salt solutions, a further shift of the IEP towards a higher pH value is recognized. If we further compare the results to the *KCl* measurements, which represent the initial membrane charge without any ion interaction, the zeta potential profiles of single salt solutions and binary mixtures show a remarkable interaction between indium and germanium ions and the membrane surface charge. Apparently, single salt solutions as well as binary mixtures of indium and germanium ions lead to enhanced specific adsorption of cations at the membrane surface since the IEP is shifted towards higher pH values. The wavy segment which could be observed at the single salt experiments is again detectable between pH 4 and 5 but it is switched to more positive values of zeta potential.

Fig. 7 shows the zeta potential obtained with binary mixtures of indium and germanium ions for NP010.

Compared to KCl, which shows the expected course of the zeta potential for a polyethersulfone membrane (see Section 3.1.1), the zeta potential profile of binary mixtures of indium and germanium shows a remarkable different trend. Because KCl is regarded as inert concerning the interaction with the membrane surface, any change in the trend of the zeta potential reveal specific interaction between the utilized electrolyte solution and the membrane surface. The IEP is not reached but in a range of pH 4–6 the membrane charge is nearly neutral. The minimum zeta potential of −25 mV can be observed both at pH 3 and pH 8.2 while there is a steep increase in zeta potential from pH 3 to 4.7. At pH values larger than pH 4.7 zeta potential decreases as expected. Due to the fact that the measured zeta potential curve is not what we expect from a polyethersulfone membrane, there must be an interaction between indium and germanium and the membrane surface. The decrease in zeta potential below pH 4.5 is most likely attributed to specific adsorption of SO_4^{2-} which is contained in the feed solution and it is also added while adjusting the pH value. Because anions are less hydrated in aqueous solution compared to cations they can approach closer to the membrane surface and consequently specific adsorption of anions is enhanced [14]. The increase of zeta potential in a range of pH 4–4.5 can

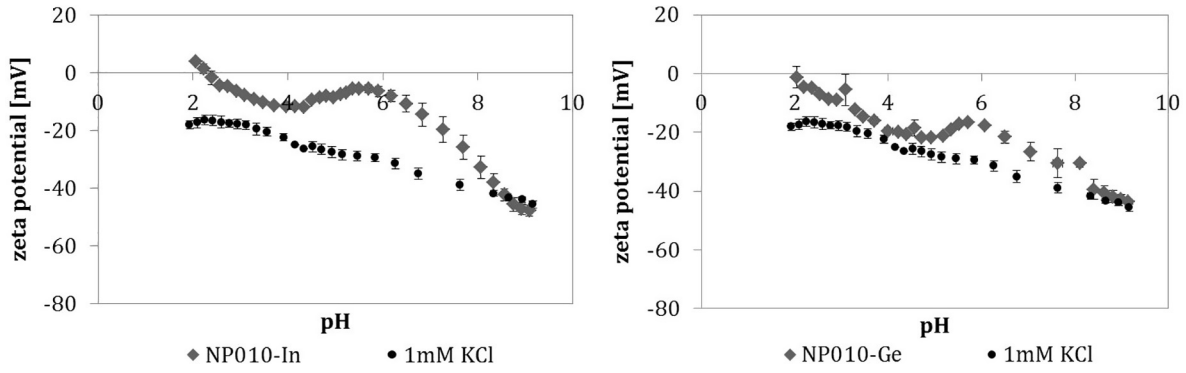

Fig. 5. NP010. Results of zeta potential measurements for single salt aqueous solutions of 10 mg l^{-1} $In_2(SO_4)_3$ (left) and 10 mg l^{-1} GeO_2 (right) compared to 1 mmol l^{-1} KCl.

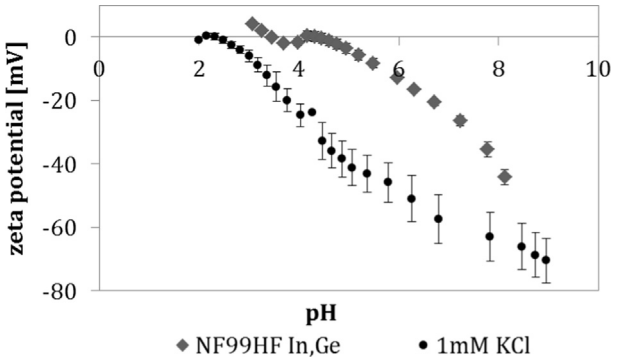

Fig. 6. NF99HF. Results of zeta potential measurements for binary mixtures of aqueous solutions containing 10 mg l^{-1} $In_2(SO_4)_3$ and 10 mg l^{-1} GeO_2 compared to 1 mmol l^{-1} KCl.

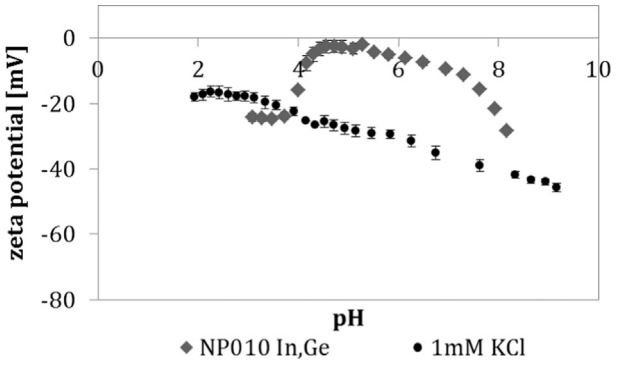

Fig. 7. NP010. Results of zeta potential measurements for binary mixtures of aqueous solutions containing 10 mg l^{-1} $In_2(SO_4)_3$ and 10 mg l^{-1} GeO_2 compared to 1 mmol l^{-1} KCl.

be related to a change of speciation (see Fig. 1) because $In(OH)_3^0$ is formed at this pH value. The formation of $In(OH)_3^0$ may lead to the formation of a passivation layer and a subsequent shielding of the membrane charge. Consequently, a net neutral charged membrane surface is acquired. With decreasing or increasing pH, indium hydroxide is dissolved and a membrane surface charge is developed. Since germanium shows a stable speciation in form of $Ge(OH)_4^0$ in the considered pH range there is no interaction with the membrane surface. It follows, that the results of zeta potential measurements are dominated by indium.

3.2. Nanofiltration experiments

The dead-end experiments with feed solutions of indium and germanium were evaluated regarding the observed ionic retention (see Eq. (2)) and the permeate flux. The flux is expressed in terms of standardized flux i.e. the ratio of the measured flux j_i at each pH value referred to the pure water flux j_{H_2O}. If the ratio j_i/j_{H_2O} is less than one, the observed permeate flux is smaller compared to the pure water flux.

3.2.1. Single salt experiments of indium and germanium - retention and permeate flux

The nanofiltration experiments with single salt solutions were investigated first due to systematic considerations. The experimental results of the observed ionic retention and the measured permeate flux for each, indium and germanium solution, are shown in Fig. 8. Error bars represent minimum and maximum deviation from the arithmetic mean. This nomenclature is consistently used for all of the following NF diagrams.

NP010. Fig. 8 displays the experimental results of single salt retention of indium and germanium and the standardized flux versus pH value, respectively.

Fig. 8 (left) shows that indium retention increases with increasing

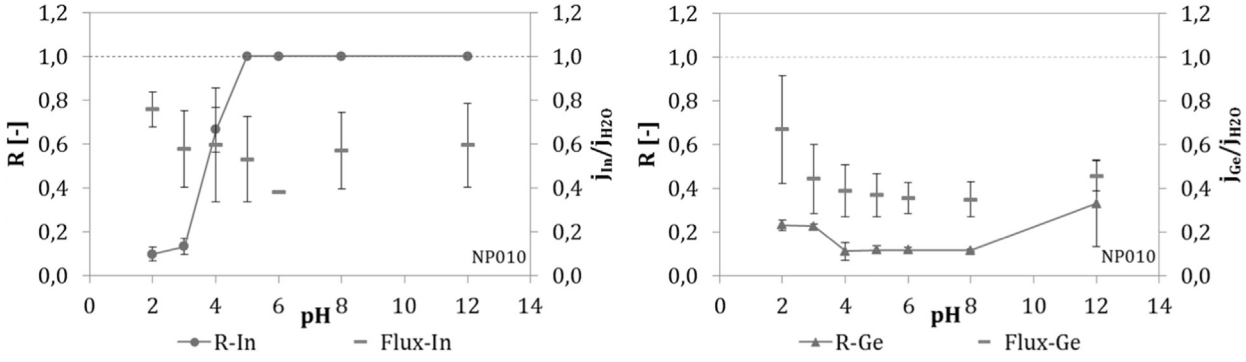

Fig. 8. NP010. Retention of single salt solutions of 10 mg l^{-1} $In_2(SO_4)_3$ (left) and 10 mg l^{-1} GeO_2 (right) and membrane performance in terms of standardized flux. (Experimental conditions: 15 bar, 25 °C, stirred batch vessel 500 rpm).

pH. The sharp increase from 0.15 to 0.65 in a pH range of 3 to 4 is well reproducible within the double determination. Referring to the speciation known from stability constants (see Fig. 1a) and measured zeta potential (Fig. 5), low retention at pH 3 is accompanied with electrostatic attraction between the negatively charged membrane surface and the hydrated In^{3+} cation. From pH 5 to 12 indium is retained close to unity which is connected to formation of $In(OH)_3^0$ and $In(OH)_4^-$. At neutral pH $In(OH)_3^0$ is the dominating species which subsequently leads to size exclusion as the dominating factor of retention. Hydroxides are also known as voluminous aggregates which enhance retention. Above pH 10 $In(OH)_4^-$ is the predominant species. With a distinct negative membrane charge, high retention at pH 12 is caused by electrostatic repulsion effects.

Referring to germanium (Fig. 8, right) there is a low retention of 0.1 in average, from pH 2 to 8. Focusing on the speciation diagram (Fig. 1b), $Ge(OH)_4^0$ dominates the speciation of germanium in a broad range until pH 8. Accordingly, size exclusion is the dominating exclusion effect. At pH 12 the majority of germanium occurs in form of $GeO(OH)_3^-$ which is supported by the experimental results regarding the negative membrane charge and increasing retention of 0.15–0.55 from pH 8 to 12.

Although indium and germanium are both uncharged at neutral pH, different separation behavior is observed. This observation must be related to a different molecular size of $Ge(OH)_4^0$ and $In(OH)_3^0$. $Ge(OH)_4^0$ is coordinated in tetrahedral structure [43] and $In(OH)_3^0$ in octahedral structure [26] (see Fig. 9). The detailed chemical structure of $In(OH)_3^0$ is indium as central ion coordinated with three OH-ligands and associated with three water molecules. Although the size of the molecule depends both on the size of the central ion and the ligands as well as on the bond length, the octahedral structure itself is a first indicator that $Ge(OH)_4^0$ is smaller compared to $In(OH)_3^0$.

In addition, In^{3+} and Ge^{4+} show remarkable differences regarding their ionic radii (see Table 2) since Ge^{4+} is half the size of In^{3+}. The ionic size is directly connected to the surface charge density (see Eq. (3)) [44]

$$\sigma_i = \frac{z_i e}{4\pi r_i^2} \tag{3}$$

where z_i is the charge number of the ion, e is the elemental charge and r_i is the ionic radius. According to Eq. (3), the surface charge density is proportional to the charge number of the ion and indirect proportional to the size of the ions.

Consequently, Ge^{4+} shows a much higher surface charge density (see Table 2) due to its smaller size and an additional positive charge, compared to In^{3+}. This leads to stronger attractive forces inside the molecule and subsequently must result in a smaller size of $Ge(OH)_4^0$, which is finally able to pass the membrane.

There are further approaches within the research project to determine diffusion coefficients of indium and germanium which would allow calculating stokes radii of indium and germanium. Furthermore, research work is done to determine the bond length of Ge—O in aqueous solution, so the calculation of the molecular size of $Ge(OH)_4^0$ would be possible. Once the mentioned data are obtained a closer consideration

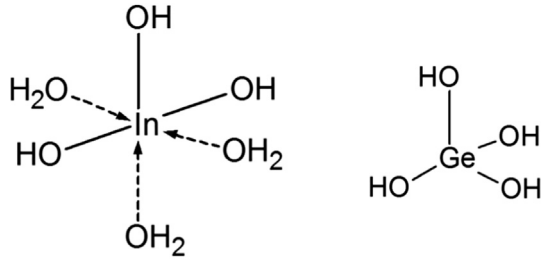

a) $[In(H_2O)_3(OH)_3]^0$ b) $Ge(OH)_4^0$

Fig. 9. Chemical structure of $In(OH)_3^0$ and $Ge(OH)_4^0$ [26,43].

Table 2
Ionic radii and surface charge density of indium and germanium [45].

Ion	r_i [Å]	σ_i [C m^{-2}]
In^{3+}	0.8[a]	5.98
Ge^{4+}	0.39[b]	33.53

[a] Octahedral coordination.
[b] Tetrahedral coordination.

of the separation mechanisms of indium and germanium is possible.

Regarding the permeate flux of indium and germanium solution (Fig. 8), a massive flux decrease with increasing pH value can be observed. These results are independent whether a solution of indium or germanium salt is considered. In case of indium, flux decreases by 20% at pH 2. The flux decreases to an average of 50% compared to pure water flux, when pH is increased. This behavior is caused by increasing osmotic pressure due to pH adjustment and a subsequent increase in ionic strength. Furthermore, there is also precipitation of $In(OH)_3^0$. Because of the high MWCO of the NP010 membrane (1000 Da), we assume that the precipitates are transported into the membrane structure and cause an irreversible scaling inside the membrane pores but further investigations have to be done. Regarding $Ge(OH)_4^0$ there is a stronger flux decrease compared to indium, which is not fully understood to date. In a range between pH 3 and 12 the flux is only 40% of the pure water flux. Since the retention of $Ge(OH)_4^0$ is much lower compared to $In(OH)_3^0$, a higher permeate flux of $Ge(OH)_4^0$ was expected.

NF99HF. Fig. 10 shows the experimental results of single salt retention of indium (left) or germanium (right) and standardized flux versus pH value.

The results of indium and germanium retention (Fig. 10) show a similar tendency compared to NP010. At pH 2, indium retention is 0.15 in average and by increasing pH value, retention increases. The retention behavior at pH 2 is not in accordance with a positive value of zeta potential (Fig. 4). Above pH 2 there is a continuous increase in retention. The high variation at pH 3 can be related to the speciation of indium since $In(OH)^{2+}$ is formed. Furthermore the IEP is located at pH 3.1 (Fig. 4) so small variations in pH value result in a considerable change in retention due to a changing membrane charge. Above pH 4 retention increases up to 1 which is consistent with the occurrence of $In(OH)_3^0$ and a subsequent size exclusion. Like NP010, high retention of indium at pH 12 is related to the negative membrane charge and electrostatic repulsion effects with the occurring $In(OH)_4^-$.

Similar to the results of NP010, retention of germanium is low and ranges from 0.2 to 0.35 between pH 2 and 8. Since the uncharged $Ge(OH)_4^0$ is the predominating species, steric retention is the dominating separation effect. Compared to NP010, NF99HF shows a smaller MWCO of 200 Da (see Table 1). Consequently, $Ge(OH)_4^0$ must be even smaller otherwise the low retention could not be observed. At pH 12 retention increases up to 0.7 which is in accordance with the net negative membrane charge (Fig. 4) and the predominant negatively charged germanium species, namely $GeO(OH)_3^-$ (Fig. 1b).

Referring to the permeate flux (Fig. 10) of the salt solutions, NF99HF also shows a flux decrease within the experimental series. Regarding the indium permeate flux a continuous decrease is observed. At neutral pH the permeate flux is 60% compared to the pure water flux. This result can be related to a combination of increasing ionic strength due to pH adjustment as well as precipitation of $In(OH)_3^0$. Due to the smaller MWCO of the NF99HF, scaling on the membrane surface and not inside the membrane pores is expected. Considering the permeate flux of germanium solution, the flux decreased by 20% compared to the pure water flux which is attributed to the increasing ionic strength. This is also in accordance with the results of the indium permeate flux since due to the precipitation of $In(OH)_3^0$ the indium permeate flux must experience a stronger decrease.

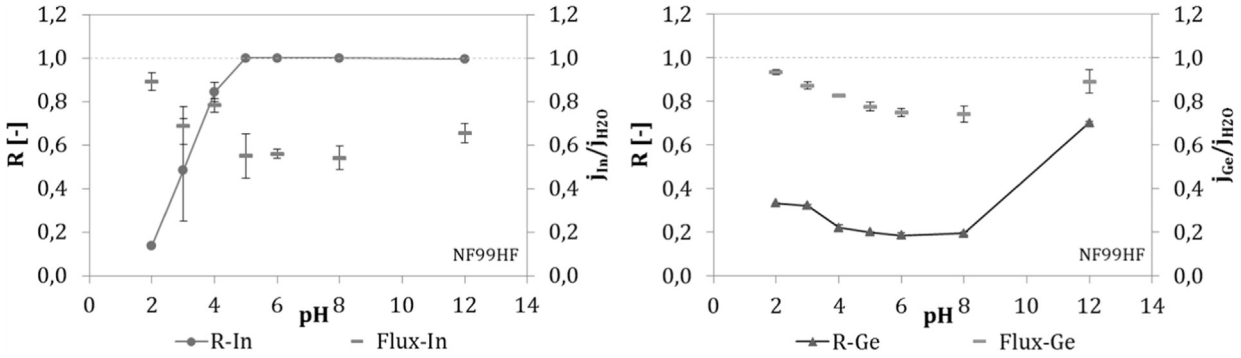

Fig. 10. NF99HF. Retention of single salt solutions of 10 mg l^{-1} $In_2(SO_4)_3$ and 10 mg l^{-1} GeO_2 and membrane performance in terms of standardized flux. (Experimental conditions. 15 bar, 25 °C, stirred batch vessel 500 rpm).

3.2.2. Binary salt mixtures of indium and germanium - retention and permeate flux

In order to investigate the influence of ionic interactions between indium and germanium, membrane experiments with binary salt mixtures of indium and germanium were performed.

NP010. Fig. 11 shows the experimental results of binary salt mixtures of indium and germanium versus pH value and the corresponding results of standardized flux referring to pure water flux for NP010.

In the binary salt mixture indium retention is characterized by a low retention of 0.15–0.3 in a range of pH 2–4 and a subsequent increase in retention above pH 4. Low retention at acidic pH values is in good agreement with indium speciation In^{3+} (Fig. 1a) and zeta potential measurements (Fig. 7) which obtained a negative membrane charge. With increasing pH value there is a steep increase in retention. In principle, the trend of the retention curve is similar to the single salt experiment (see Fig. 8). Unlike the single salt experiments, the increase in retention is shifted towards pH > 4 which is consequently related to speciation phenomena of simultaneously occurring indium and germanium since all the other parameters remained unchanged. Above pH 4 indium retention is 0.95–1 which is related to size exclusion of $In(OH)_3^0$ from pH 5–10 and subsequent electrostatic repulsion of $In(OH)_4^-$ and the negative membrane surface charge above pH 10 (Fig. 7). As results show, in a pH range of pH 5–12 indium is effectively separated from germanium.

The retention of germanium is low in a range between 0.1 and 0.2 for all investigated pH values from pH 2 to 12 (Fig. 11). Retention behavior is comparable to the single salt experiments (Fig. 8) except at pH 12, since now retention is lower by more than 50%. This observation is most likely associated to the Donnan effect. At pH 12 the speciation of indium and germanium is dominated by $In(OH)_4^-$ and $GeO(OH)_3^-$ and the membrane has a negative membrane charge (Fig. 7). The occurring Na^+ ions (pH adjustment) will experience electrostatic attraction, so passing of $GeO(OH)_3^-$ is necessary to maintain electro neutral conditions in the permeate solution. Furthermore, as a result of the calculation of the surface charge density (Table 2) the assumption of $GeO(OH)_3^-$ being smaller compared to $In(OH)_4^-$ is justified. Consequently, in a binary mixture of indium and germanium, germanium does not show a pH dependent separation behavior with NP010 and hence is concentrated in the permeate solution.

The permeate flux of the binary salt solution (Fig. 11) shows similar results compared to the single salt experiments (Fig. 8) which again is an effect of increasing osmotic pressure due to pH adjustment and the precipitation of $In(OH)_3^0$ which most likely cause scaling inside the membrane pores. Accordingly, in the binary mixture of indium and germanium the membrane performance of NP010 in terms of permeate flux is dominated by the presence of indium.

NF99HF. Fig. 12 shows the experimental results of binary salt mixtures of indium and germanium and the corresponding results of standardized flux depending on pH value.

Within the binary salt system indium retention is in a range of 0.8 at pH 2 and 3. With increasing pH, retention increases to 1 in a range of pH 5–12. Compared to the single salt measurements (Fig. 10) differences are observable in terms of increasing indium retention by 80% at pH 2. This observation is in accordance with the positive membrane charge at pH 2 (Fig. 6) and hence the occurring electrostatic repulsion between In^{3+} and the positively charged membrane surface.

Germanium retention is low in a range of 0.15–0.2 between pH 2 and 8. At pH 12, retention increases to an average of 0.5 but results show high variation. The experiment at pH 12 was repeated five times to check whether the deviation is random or not. After several runs the deviation was confirmed whereas indium was constantly retained with 0.99 for all experiments. Although both membranes show negative surface charge at pH 12 there are differences in retention which is due to the different MWCO of NF99HF and NP010. Similarly to NP010, the

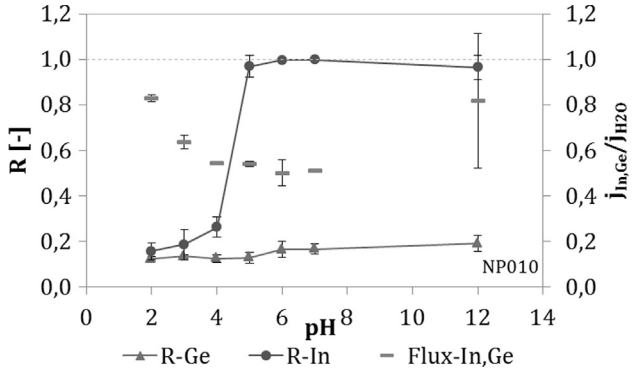

Fig. 11. NP010. Retention of binary salt mixtures of 10 mg l^{-1} $In_2(SO_4)_3$ and 10 mg l^{-1} GeO_2 and membrane performance in terms of standardized flux. (Experimental conditions: 15 bar, 25 °C, stirred batch vessel 500 rpm).

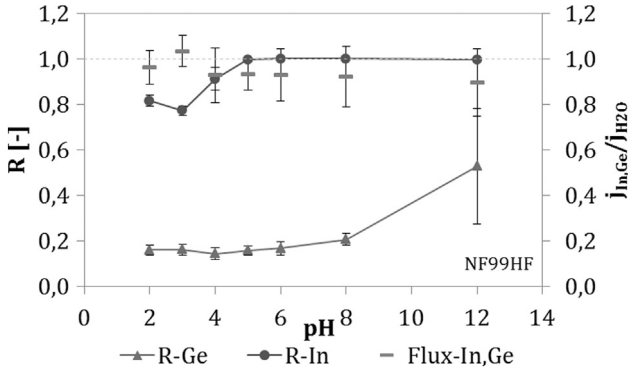

Fig. 12. NF99HF. Retention of binary salt mixtures of 10 mg l^{-1} $In_2(SO_4)_3$ and 10 mg l^{-1} GeO_2 and membrane performance in terms of standardized flux. (Experimental conditions: 15 bar, 25 °C, stirred batch vessel 500 rpm).

NF99HF membrane also reveals a negative membrane charge at pH 12. So again, the Donnan effect is assumed to be the effective separation mechanisms (see above). But since the MWCO of the NF99HF is smaller (200 Da) compared to NP010 (1000 Da), there is an additional size exclusion effect which enhances the retention of $GeO(OH)_3^-$. Finally the results show, that the treatment with NF99HF also enables a selective separation of indium and germanium between pH 2 and 8, while germanium is enriched in the permeate.

Referring to membrane performance it can be seen that the flux of the binary salt mixtures is remarkably higher compared to the flux obtained with the single salt solutions (Fig. 10). There is an average flux decrease of 10% referring to pure water flux. Furthermore, a constant performance loss with ongoing experiments is not observed. This observation is not in accordance with our expectations, because due to an increase in ionic strength a curve at least similar to the single salt experiments was expected.

Comparing NP010 and NF99HF, there is a stronger decrease of permeate flux for NP010 due to a larger effective pore radius compared to NF99HF. Since this observation occurred in a pH range where indium hydroxide is predominant, the hypothesis of irreversible scaling inside the membranes pores of NP010 (see Section 3.2.1) is supported.

4. Conclusions

In the present study, the pH dependent separation of indium and germanium was investigated by means of nanofiltration. Two polymeric nanofiltration membranes (NF99HF, NP010) made of different membrane material were used and the experiments were performed in dead end filtration mode (Experimental conditions: 15 bar, 25 °C, stirred batch vessel 500 rpm). The dead-end experiments with single salt solutions and binary mixtures of indium and germanium were evaluated regarding observed ionic retention as well as standardized flux.

In a binary salt mixture of $In_2(SO_4)_3$ and GeO_2, indium and germanium can be separated from one another by variation of pH value. This is on the one hand related to a change of speciation and on the other hand related to a change of membrane charge due to a variation of pH value in a range of pH 2–12. The results showed that in a future technical application, germanium is enriched in the permeate. Experiments with single salt solutions and binary salt mixtures of $In_2(SO_4)_3$ and GeO_2 revealed differences in retention which is related to ion-membrane interaction in terms of electrostatic interaction and size exclusion.

To evaluate the effect of indium and germanium ions on value and sign of the membrane charge, the pH dependent zeta potential of the membrane surface was determined by measuring the streaming potential. KCl was used as a reference system because it is inert regarding membrane surface interaction. Compared to the experiments performed with KCl, zeta potential profiles of single salt solutions and binary mixtures of indium and germanium showed a remarkable interaction between indium and germanium ions and the membrane surface charge since the IEP was shifted towards higher pH values. This result indicates the specific adsorption of cations, namely In^{3+}.

Streaming potential measurements with binary mixtures of $In_2(SO_4)_3$ and GeO_2 to determine zeta potential showed an IEP of 3.5 for NF99HF. In case of NP010, zeta potential showed a negative membrane charge throughout the entire investigated pH range with a distinct increase in zeta potential from 4 to 4.5 and subsequent decrease which is untypical for polymeric membranes. The differences observed in zeta potential must be accompanied by the interaction of membrane material and speciation. As results show, NP010 shows strong interaction with the electrolyte solution containing indium and germanium.

The qualitative assessment of the experiments in terms of standardized flux i.e. measured ionic permeate flux referred to pure water flux also revealed distinct differences between NP010 and NF99HF. Finally, when treating the more complex binary salt solution, NF99HF showed a remarkable higher permeate flux.

The present results suggest complex interaction of different phenomena such as membrane-solution interaction as well as interaction of pH-dependent species with the membrane and among each other. Still, clarification of the underlying separation mechanisms and prediction of membrane performance with respect to flux and retention of involved ionic species remains difficult. Further experimental investigation will increase complexity of the ionic solution to evaluate ionic interaction. Furthermore experiments in cross flow filtration mode will be performed to assess the influence of changed hydrodynamic conditions. There are also further approaches within the current research work to determine diffusion coefficients of indium and germanium as well as the bond length of Ge—O in aqueous solution, so the calculation of the molecular size of $Ge(OH)_4^0$ would be possible. Once the mentioned data are obtained a closer consideration of the separation mechanisms of indium and germanium is possible.

Acknowledgement

We thank the Dr.-Erich-Krüger Foundation for the financial support. Thanks also go to Dipl.-Min. Ulrike Fischer from TU Bergakademie Freiberg (Germany) and Helmholtz Centre for Environmental Research (UFZ) for determining the indium and germanium concentrations in the sample solutions via ICP-MS.

We thank the Research Institute of Leather and Plastic Sheeting (FILK) for running the zeta potential measurements.

Special thanks go to Prof. Gero Frisch and M.Chem. Charlotte Ashworth from TU Bergakademie Freiberg (Germany) for providing detailed knowledge of the speciation chemistry of indium and germanium.

References

[1] European Commission, Critical raw materials for the EU: Report of the ad-hoc working group on defining critical raw materials, 2014.
[2] G. Gunn, Critical metals handbook, British Geological Survey; Wiley; American Geophysical Union, Chichester, 2014.
[3] USGS National Minerals Information Center, Germanium: Minerals Yearbook, 2015, accessed 13 September 2017.
[4] USGS National Minerals Information Center, Indium: Minerals Yearbook, 2015, accessed 13 September 2017.
[5] A.M. Alfantazi, R.R. Moskalyk, Processing of indium: a review, Min. Eng. 16 (2003) 687–694.
[6] R.R. Moskalyk, Review of germanium processing worldwide, Min. Eng. 17 (2004) 393–402.
[7] N.J. Cook, C.L. Ciobanu, A. Pring, W. Skinner, M. Shimizu, L. Danyushevsky, B. Saini-Eidukat, F. Melcher, Trace and minor elements in sphalerite: a LA-ICPMS study, Geochim. Cosmochim. Acta 73 (2009) 4761–4791.
[8] H.R. Watling, The bioleaching of sulphide minerals with emphasis on copper sulphides – a review, Hydrometallurgy 84 (2006) 81–108.
[9] S.M.C. Santos, R.M. Machado, M.J.N. Correia, M.T.A. Reis, M.R.C. Ismael, J.M.R. Carvalho, Ferric sulphate/chloride leaching of zinc and minor elements from a sphalerite concentrate, Min. Eng. 23 (2010) 606–615.
[10] A. Schippers, W. Sand, Bacterial leaching of metal sulfides proceeds by two indirect mechanisms via thiosulfate or via polysulfides and sulfur, Appl. Environ. Microbiol. 65 (1999) 319–321.
[11] W.R. Bowen, H. Mukhtar, Characterisation and prediction of separation performance of nanofiltration membranes, J. Membr. Sci. 112 (1996) 263–274.
[12] S. Bandini, J. Drei, D. Vezzani, The role of pH and concentration on the ion rejection in polyamide nanofiltration membranes, J. Membr. Sci. 264 (2005) 65–74.
[13] M.R. Teixeira, M.J. Rosa, M. Nyström, The role of membrane charge on nanofiltration performance, J. Membr. Sci. 265 (2005) 160–166.
[14] A.E. Childress, M. Elimelech, Effect of solution chemistry on the surface charge of polymeric reverse osmosis and nanofiltration membranes, J. Membr. Sci. 119 (1996) 253–268.
[15] M. Elimelech, W.H. Chen, J.J. Waypa, Measuring the zeta (electrokinetic) potential of reverse osmosis membranes by a streaming potential analyzer, Desalination 95 (1994) 269–286.
[16] S. Bandini, C. Mazzoni, Modelling the amphoteric behaviour of polyamide nanofiltration membranes, Desalination 184 (2005) 327–336.
[17] J. Tanninen, M. Nyström, Separation of ions in acidic conditions using NF, Desalination 147 (2002) 295–299.
[18] G. Hagmeyer, R. Gimbel, Modelling the salt rejection of nanofiltration membranes for ternary ion mixtures and for single salts at different pH values, Desalination 117 (1998) 247–256.
[19] M. Ernst, A. Bismarck, J. Springer, M. Jekel, Zeta-potential and rejection rates of a polyethersulfone nanofiltration membrane in single salt solutions, J. Membr. Sci. 165 (2000) 251–259.

[20] L. Bruni, S. Bandini, The role of the electrolyte on the mechanism of charge formation in polyamide nanofiltration membranes, J. Membr. Sci. 308 (2008) 136–151.
[21] J.-J. Qin, M.H. Oo, H. Lee, B. Coniglio, Effect of feed pH on permeate pH and ion rejection under acidic conditions in NF process, J. Membr. Sci. 232 (2004) 153–159.
[22] L. Sigg, W. Stumm, Aquatische Chemie: Einführung in die Chemie natürlicher Gewässer, 5th ed., Zürich: vdf, Hochschulverl. ETH Zürich, 2011.
[23] IUPAC, Guidelines for terms related to chemical speciaiton and fractionation of elements. Definitions, structural aspects and methodological approaches: IUPAC Recommendations 2000, Pure Appl. Chem. 72 (2000) 1453–1470.
[24] C.F. Baes, R.E. Mesmer, The hydrolysis of cations, Krieger Publishing Company, Malabar, Florida, 1986.
[25] HySS - Hyperquad Simulation and Speciation, 2009, http://www.hyperquad.co.uk/.
[26] S.A. Wood, I.M. Samson, The aqueous geochemistry of gallium, germanium, indium and scandium, Ore Geol. Rev. 28 (2006) 57–102.
[27] G.S. Pokrovski, J. Schott, Thermodynamic properties of aqueous Ge(IV) hydroxide complexes from 25 to 350 °C: implications for the behavior of germanium and the Ge/Si ratio in hydrothermal fluids, Geochim. Cosmochim. Acta 62 (1998) 1631–1642.
[28] M. Hoyer, D. Zabelt, R. Steudtner, V. Brendler, R. Haseneder, J.-U. Repke, Influence of speciation during membrane treatment of uranium contaminated water, Sep. Puri. Tech. 132 (2014) 413–421.
[29] S. Bouranene, P. Fievet, A. Szymczyk, M.E.H. Samar, A. Vidonne, Influence of operating conditions on the rejection of cobalt and lead ions in aqueous solutions by a nanofiltration polyamide membrane, J. Membr. Sci. 325 (2008) 150–157.
[30] C.V. Gherasim, J. Cuhorka, P. Mikulásek, Analysis of lead(II) retention from single salt and binary aqueous solutions by a polyamide nanofiltration membrane Experimental results and modelling, J. Membr. Sci. 436 (2013) 132–144.
[31] M. Wu, D.D. Sun, J.H. Tay, Effect of operating variables on rejection of indium using nanofiltration membranes, J. Membr. Sci. 240 (2004) 105–111.
[32] A. Werner, M. Mosch, R. Haseneder, J.-U. Repke, Selektive Abtrennung von Indium und Germanium aus Laugungslösungen mit Membranverfahren, Chem. Ing. Tech. 87 (2015) 1826–1832.
[33] A. Werner, R. Haseneder, J.-U. Repke, Membrangestützte Verfahren zur selektiven Abtrennung von Indium und Germanium aus Laugungslösungen, Chemie Ingenieur Technik 87 (2015) 1088–1089.
[34] Alfa Laval, Alfa Laval NF series – Spiral membranes for nanofiltration: Product data sheet, 2013.
[35] Microdyn Nadir, The art to clear solutions, Product Catalog, 2014.
[36] D.L. Oatley, L. Llenas, R. Pérez, P.M. Williams, X. Martínez-Lladó, M. Rovira, Review of the dielectric properties of nanofiltration membranes and verification of the single oriented layer approximation, Adv. Coll. Interface. Sci. 173 (2012) 1–11.
[37] K.Y. Wang, T.-S. Chung, The characterization of flat composite nanofiltration membranes and their applications in the separation of Cephalexin, J. Membr. Sci. 247 (2005) 37–50.
[38] A.L. Carvalho, F. Maugeri, V. Silva, A. Hernández, L. Palacio, P. Pradanos, AFM analysis of the surface of nanoporous membranes: application to the nanofiltration of potassium clavulanate, J. Mater. Sci. 46 (2011) 3356–3369.
[39] M. Mänttäri, A. Pihlajamäki, M. Nyström, Effect of pH on hydrophilicity and charge and their effect on the filtration efficiency of NF membranes at different pH, J. Membr. Sci. 280 (2006) 311–320.
[40] T. Luxbacher, The Zeta Guide: Principles of the streaming potential technique, Anton Paar GmbH, 2014.
[41] S. Bandini, Modelling the mechanism of charge formation in NF membranes: theory and application, J. Membr. Sci. 264 (2005) 75–86.
[42] J. Schaep, C. Vandecasteele, Evaluation the charge of nanofiltration membranes, J. Membr. Sci. 188 (2001) 129–136.
[43] N. Ingri, Equilibrium studies of polyanions: 12. Polygermanates in Na(Cl) medium, Acta Chemica Scandinavica 17 (1963) 597–616.
[44] E. Mauerhofer, K. Zhernosekov, F. Rösch, Limiting transport properties of lanthanide and actinide ions in pure water, Radiochim. Acta 91 (2003) 473–477.
[45] R.D. Shannon, Revised effective ionic radii and systematic studies of interatomie distances in halides and chaleogenides, Acta Crystallogr. Sect. A 32 (1976) 751–767.